#### RESEARCH ARTICLE





### The gut-brain axis in individuals with alcohol use disorder: An exploratory study of associations among clinical symptoms, brain morphometry, and the gut microbiome

Katherine A. Maki<sup>1</sup> | Gwenyth R. Wallen<sup>1</sup> | Thomaz F. S. Bastiaanssen<sup>2</sup> | Li-Yueh Hsu<sup>3</sup> | Michael E. Valencia<sup>1</sup> | Vijay A. Ramchandani<sup>4</sup> | Melanie L. Schwandt<sup>4</sup> | Nancy Diazgranados<sup>4</sup> | John F. Cryan<sup>2</sup> | Reza Momenan<sup>5</sup> | Jennifer J. Barb<sup>1</sup>

#### Correspondence

Katherine A. Maki, National Institutes of Health, Building 10 Rm 2B10, 10 Center Drive, Bethesda, MD 20814, USA. Email: katherine.maki@nih.gov

#### **Funding information**

NIH Clinical Center, Grant/Award Number: Z99CL999999

#### **Abstract**

Background: Alcohol use disorder (AUD) is commonly associated with distressing psychological symptoms. Pathologic changes associated with AUD have been described in both the gut microbiome and brain, but the mechanisms underlying gut-brain signaling in individuals with AUD are unknown. This study examined associations among the gut microbiome, brain morphometry, and clinical symptoms in treatment-seeking individuals with AUD.

Methods: We performed a secondary analysis of data collected during inpatient treatment for AUD in subjects who provided gut microbiome samples and had structural brain magnetic resonance imaging (MRI; n = 16). Shotgun metagenomics sequencing was performed, and the morphometry of brain regions of interest was calculated. Clinical symptom severity was quantified using validated instruments. Gut-brain modules (GBMs) used to infer neuroactive signaling potential from the gut microbiome were generated in addition to microbiome features (e.g., alpha diversity and bacterial taxa abundance). Bivariate correlations were performed between MRI and clinical features, microbiome and clinical features, and MRI and microbiome features. Results: Amygdala volume was significantly associated with alpha diversity and the abundance of several bacteria including taxa classified to Blautia, Ruminococcus, Bacteroides, and Phocaeicola. There were moderate associations between amygdala volume and GBMs, including butyrate synthesis I, glutamate synthesis I, and GABA synthesis I & II, but these relationships were not significant after false discovery rate (FDR) correction. Other bacterial taxa with shared associations to MRI features and clinical symptoms included Escherichia coli and Prevotella copri.

Conclusions: We identified gut microbiome features associated with MRI morphometry and AUD-associated symptom severity. Given the small sample size and bivariate associations performed, these results require confirmation in larger samples

Reza Momenan and Jennifer J. Barb are co-senior authors.

This is an open access article under the terms of the Creative Commons Attribution License, which permits use, distribution and reproduction in any medium, provided the original work is properly cited.

© 2024 The Author(s). Alcohol, Clinical and Experimental Research published by Wiley Periodicals LLC on behalf of Research Society on Alcohol. This article has been contributed to by U.S. Government employees and their work is in the public domain in the USA.

<sup>&</sup>lt;sup>1</sup>Translational Biobehavioral and Health Disparities Branch, National Institutes of Health, Clinical Center, Bethesda, Maryland, USA

<sup>&</sup>lt;sup>2</sup>APC Microbiome Ireland and Department of Anatomy & Neuroscience, University College Cork, Cork, Ireland

<sup>&</sup>lt;sup>3</sup>Radiology and Imaging Sciences, National Institutes of Health, Clinical Center, Bethesda, Maryland, USA

<sup>&</sup>lt;sup>4</sup>National Institute on Alcohol Abuse and Alcoholism, National Institutes of Health, Bethesda, Maryland, USA

<sup>&</sup>lt;sup>5</sup>Clinical NeuroImaging Research Core, National Institute on Alcohol Abuse and Alcoholism, National Institutes of Health, Bethesda, Maryland, USA

29937175, 2024, 7, Downloaded from https://onlinelibrary.wiley.com/doi/10.1111/acer.15346 by Nat Prov Indonesia, Wiley Online Library on [16/07/2024]. See the Terms

and Conditions (https

and-conditions) on Wiley Online Library for rules

of use; OA

articles are governed by the

applicable Creative Commons

and controls to provide meaningful clinical inferences. Nevertheless, these results will inform targeted future research on the role of the gut microbiome in gut-brain communication and how signaling may be altered in patients with AUD.

#### **KEYWORDS**

addiction, alcohol use disorder, gastrointestinal microbiome, gut-brain axis, neuroimaging

#### INTRODUCTION

The misuse of alcohol is a global public health concern that compromises both individual and societal well-being, resulting in an estimated three million deaths annually (World Health Organization, 2019). Alcohol use disorder (AUD) is a highly prevalent disease, and approximately one-third of the United States adult population has met the Diagnostic and Statistical Manual of Mental Disorders-5 (DSM-5) criteria for AUD at some point in their lives (Witkiewitz et al., 2019). AUD is considered to be mainly a disorder of the brain reward circuit where alterations in neurotransmitter systems such as dopamine, serotonin and glutamate, among others, are associated with the positive and negative reinforcement processes leading to craving for alcohol and increased dependence over time (Gilpin & Koob, 2008).

Chronic heavy alcohol use and AUD are associated with many distressing symptoms including symptoms of anxiety and depression, sleep disruption, and altered stress handling (Wallen et al., 2019). Altered basal plasma cortisol levels, often seen in patients with AUD, are associated with similar symptoms including sleep changes, symptoms of depression and anxiety, as well as immune upregulation and inflammation (Fiksdal et al., 2019; Leclercq. De Saeger, et al., 2014). Alcohol-induced inflammation and neuroendocrine dysregulation may have multifactorial implications for patients with AUD including exacerbation of common symptoms (i.e., craving, withdrawal, anxiety, depression, and sleep disturbance), increased risk of relapse, and compounded risk for chronic disease (Rohleder, 2019). Gastrointestinal manifestations are also common complaints in patients with AUD (Bishehsari et al., 2017), which are likely associated with implications of chronic alcohol consumption including alteration of the gastrointestinal environment and the gut microbiome (Bishehsari et al., 2017; Leclercg, Matamoros, et al., 2014).

The human gut microbiome is defined as the commensal gut bacteria that live within and coexist with humans (and their genes). Gut microbiome bacteria perform vital physiologic functions such as immune regulation, nutrient metabolism, and production of signaling metabolites like short-chain fatty acids (Belkaid & Harrison, 2017; Silva et al., 2020). Heavy alcohol consumption induces profound changes in the gastrointestinal environment including lower pH of feces and increased gut permeability (Engen et al., 2015; Leclercq et al., 2012; Leclercq, Matamoros, et al., 2014) that is associated with the translocation of microbial byproducts and mediators from the gastrointestinal environment into the intestinal lumen and systemic circulation (Ferro et al., 2020). Heavy

alcohol use and AUD have been associated with pathologic changes in the gut microbiome including decreased commensal bacteria (i.e. *Lactobacillus*, *Bifidobacterium*), reduced microbial diversity, and increased inflammatory bacteria like Proteobacteria (Ames et al., 2020; Leclercq, Matamoros, et al., 2014). Furthermore, inflammatory pathways were more intensively activated by lipopolysaccharide and peptidoglycan exposure in cells from subjects with AUD versus nondrinking controls, suggesting chronic alcohol exposure primes subjects for microbiome-induced inflammation (Leclercq, De Saeger, et al., 2014).

Interoceptive signaling of gut microbiome-associated mediators and metabolites to the brain, known as microbiota-gut-brain axis signaling, is hypothesized to occur through a number of mechanisms, including microbiome-derived metabolites, microbiome-immune crosstalk, and afferent gastrointestinal signaling mediated by the vagus nerve and enteric nervous system (Bassett et al., 2019; Cryan et al., 2019; Wang et al., 2018). Recent research also suggests bacterial communities of the gut microbiome can influence brain function and behavioral phenotype and may be associated with the pathogenesis of psychiatric disorders such as AUD (Carbia et al., 2021; Dinan & Cryan, 2017). Preclinical research has also shown that the gut microbiome can influence the key neural pathways implicated in AUD clinical manifestations and HPA axis alterations. For example, germ-free mice have marked changes in brain regions associated with anxiety- and depressive-like symptoms including amygdalar (Stilling et al., 2015), hippocampal (Clarke et al., 2013), and cortical (Hoban et al., 2016) gene expression in addition to an exaggerated HPA axis response corresponding to changes in anxiety, cognitive, and social behaviors (Luczynski et al., 2016). Although there is compelling evidence that sustained alcohol use induces inflammatory and stress-signaling mechanisms associated with symptom burden in AUD, the mechanisms and links to the known altered stress responses in patients with AUD are still being explored.

AUD is a heterogeneous condition that is incredibly difficult to manage, and pharmacological treatment modalities have limited efficacy (Heilig et al., 2019; Volkow et al., 2015). There is a critical need to identify alternative targets that can be studied in the context of AUD. In 2019, Valles-Colomer and colleagues developed a database of gut-brain signaling pathways, called gut-brain modules (GBMs), that are informed by the literature and calculated from shotgun metagenomics sequencing data (Valles-Colomer et al., 2019). GBMs describe the synthesis and degradation of neuroactive compounds by the gut microbiota and therefore allow for the assessment of specific processes relevant to gut-brain communication from sets or pathways of genes rather than singular

genes. This enables more precise and reliable interrogation of gutbrain communication versus interrogating what is achievable with single genes. Understanding microbially derived features and their associated signaling processes hold promise for nonpharmacologic interventions, but concrete mechanisms linking the microbiome to neurologic outcomes (brain morphometry or symptom severity) have yet to be determined in patients with AUD. Therefore, research focused on investigating relationships between bacterial and functional features specific to the gut microbiome, brain morphometry from structural magnetic resonance imaging (MRI), and clinical symptoms may provide the necessary preliminary information to inform future targeted mechanistic studies aimed at addressing this knowledge gap. The objective of this exploratory secondary analysis study was to examine associations between the gut microbiome, structural MRI morphometry, and severity of AUD-associated clinical symptoms in treatment-seeking patients with AUD.

#### **METHODS**

#### Study overview

This is a secondary analysis that incorporated shotgun sequencing of previously collected gut microbiome samples from individuals with AUD during an inpatient treatment program at the National Institutes of Health Clinical Center. The primary work from this study included a longitudinal experimental design using 16S rRNA sequencing of oral and gut microbiome samples from patients undergoing inpatient treatment for AUD (Ames et al., 2020; Barb et al., 2022). The original study and this secondary analysis were approved by the National Institutes of Health Institutional Review Board (NCT02911077) and primary data collection was conducted over approximately 1 year (2016-2017). Eligibility and clinical baseline measures were established via the National Institutes of Health-approved National Institute on Alcohol Abuse and Alcoholism natural history and research protocol (NCT02231840). This secondary analysis includes previously collected clinical data and structural MRI imaging measures that were analyzed with stored fecal samples that underwent shotgun metagenomics sequencing to explore relationships between the gut microbiome, morphometry of brain regions associated with the HPA-axis, and clinical phenotype variables in treatment-seeking patients with AUD (Figure 1). Please see Ames et al. (2020), for full screening procedures, inclusion and exclusion criteria, and the primary study procedures.

#### Study population

A total of 16 treatment-seeking individuals with AUD enrolled at the NIH Clinical Center inpatient treatment program who had gut microbiome samples collected and structural MRI imaging performed

during the four-week inpatient treatment period were studied (Figure 1A).

#### Clinical measures

Clinical measures encompassing alcohol use, intake history, and subjective symptoms of anxiety, depression, sleep quality, craving for alcohol, and withdrawal were collected upon consent into the natural history protocol (See Table S1 for full description and scoring of alcohol-associated and clinical measures). To quantify drinking patterns and characterize alcohol dependence severity for study population description, the Alcohol Dependence Scale, Alcohol Use Disorder Identification Test, Obsessive Compulsive Drinking Scale, Alcohol Timeline Followback (TLFB), and Lifetime Drinking History were collected at baseline during the first-week postadmission. The Bristol stool form scale was recorded to evaluate the consistency of the fecal sample collected for microbiome analysis. Individuals with current mood and/or anxiety disorders were determined using the Structured Clinical Interview for DSM-IV or DSM-5. Participants also completed instruments quantifying symptoms of depression and anxiety (the Brief Scale for Anxiety [BSA] and Montgomery Asberg Depression Rating Scale [MADRS] subscales of the Comprehensive Psychopathological Rating Scale questionnaire, respectively), subjective sleep quality (Pittsburg Sleep Quality Index [PSQI]), craving for alcohol (Penn Alcohol Craving Scale [PACS]), and withdrawal from alcohol (Clinical Institute Withdrawal Assessment [CIWA]). The PSQI was administered on days 2 and 28 of admission, PACS at 7-day intervals starting from the fifth day of admission, and BSA/MADRS also at 7-day intervals starting from the second day of admission. Scores from the PSQI, PACS, BSA, and MADRS collected at the timepoint closest to the date of the structural MRI and microbiome sample were used for this cross-sectional analysis (Figure 1A). The daily maximum CIWA score from admission days 1-4 was collected for each patient and averaged for the quantification of alcohol withdrawal severity.

#### Nutritional dietary intake during inpatient treatment

Nutritional intake during inpatient treatment was monitored using food tickets at the NIH Clinical Center. Detailed procedures for dietary data collection and processing have been described previously (Ames et al., 2020). Briefly, food tickets accompanied each meal that presented the food components provided, and the percent of each component consumed were recorded by the subject and returned to the Clinical Center nutrition department. Food information was coded and uploaded to the Nutrition Data System for Research software (version 2016/17, Nutrition Coordinating Center, University of Minnesota). The nutritional intake data analyzed in the NDSR software was used to calculate the Health Eating Index (HEI-2015) for each patient (Reedy et al., 2018). Food tickets were analyzed on the day of and the day before the fecal

29937175, 2024, 7, Downloaded from https://onlinelibrary.wiley.com/doi/10.1111/acer.15346 by Nat Prov Indonesia, Wiley Online Library on [16/07/2024]. See the Terms and Conditions (https://onlinelibrary.wiley.com/werns/

and-conditions) on Wiley Online Library for rules of use; OA articles are governed by the applicable Creative Commons License

### **Study Design**

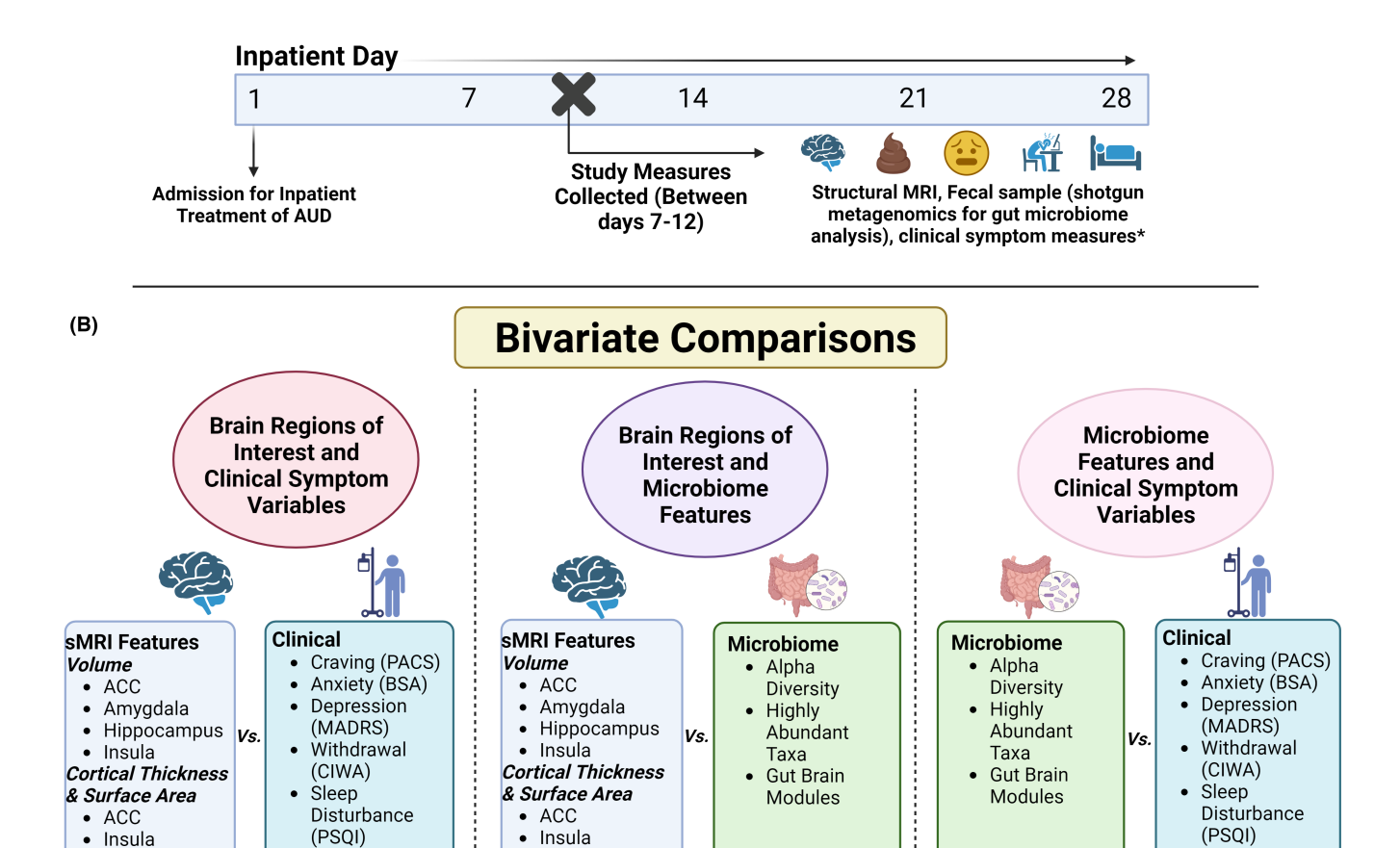


FIGURE 1 Study overview. (A) Overview of the study design. Cross sectional study measures collected from patients with AUD admitted to treatment program at the NIH Clinical Center. The fecal sample that was collected closest to the date the structural MRI was completed underwent shotgun metagenomics sequencing. (B) Schema of three comparison analyses and workflows of cross-sectional investigations of clinical and gut microbiome data. Brain regions of interest compared with clinical symptom characteristics/measures (orange bubble). Brain regions of interest compared with alpha diversity metrics, abundant taxonomic features, and gut-brain modules (purple bubble). Gut microbiome features compared with clinical symptom characteristics (pink bubble). Created with BioRender.com.

sample was collected for gut microbiome analysis, and nutritional information for those 2 days was averaged. Total kcal daily intake and average carbohydrate, protein, fat, and dietary fiber intake are reported.

#### Magnetic resonance image acquisition and processing

A whole brain structural MRI scan was obtained for volumetric and morphological analyses in this cohort of patients once during inpatient admission. MRI data were acquired on 3 Tesla Siemens Prisma (Siemens Healthineers, Erlangen, Germany; n=9) and 3 Tesla Philips Achieva (Philips Medical Systems, Best, The Netherlands; n=7) scanners. A spin echo sequence (TR 600 ms, TE 8.9 ms, flip angle 75°, NEX 1, acquisition matrix  $320 \times 224$ , slice thickness 4 mm, pixel spacing  $0.72 \times 0.72$  mm) was used in

the Siemens scanner, while a gradient echo sequence (TR  $8.2\,\text{ms}$ , TE  $3.7\,\text{ms}$ , flip angle  $8^\circ$ , NEX 1, acquisition matrix  $240\times240$ , slice thickness 1 mm, pixel spacing  $0.94\times0.94\,\text{mm}$ ) was used in the Philips scanner to acquire 3D sagittal T1-weighted anatomical images. All MR imaging was performed at the National Institutes of Health Clinical Center.

For cortical reconstruction and volumetric segmentation of the T1 brain MR images, we used FreeSurfer (http://surfer.nmr.mgh.harvard.edu) image analysis suite (v7.2) to obtain regional measures of cortical volume, surface area, and thickness. The image processing pipeline in FreeSurfer included motion correction and averaging of T1-weighted images, removal of nonbrain tissue, automated Talairach transformation, segmentation of the subcortical white matter and deep gray matter structures, intensity normalization, tessellation of the gray matter white matter boundary, automated topology correction, and surface deformation. Expanded technical

details of the FreeSurfer image processing procedures can be found in (Dale et al., 1999; Desikan et al., 2006; Fischl & Dale, 2000). After the FreeSurfer pipeline processing, parcellated morphological volume measures of the following bilateral components were quantified: amygdala, anterior cingulate cortex (ACC), hippocampus, and insula; as well as pons, brain volume (without ventricles), and brain stem for normalization procedures. Brain regions of interest (ROI) were prospectively selected due to their association with HPA-axis activity (Critchley, 2005; Quevedo et al., 2017), and well-described morphometric modulation associated with chronic alcohol use and AUD (Grace et al., 2021; Momenan et al., 2012; Yang et al., 2016). For surface area and thickness measures, the following bilateral composite regions of interest, as defined in Pennington et al. (2015), were calculated: (1) ACC includes rostral anterior cingulate and caudal anterior cingulate regions, and (2) insula. In addition, normalized volume measures were calculated by dividing each regional volume measure by the brain volume (without ventricles), and normalized surface area measures were calculated by dividing the surface area of each bilateral composite region with the white matter surface area in each hemisphere.

#### Fecal sample collection and processing

The collection, processing, and storage procedures of fecal samples for gut microbiome analysis have previously been described in detail (Ames et al., 2020). Briefly, whole stool was collected using sterile conditions from each participant upon deposition and was immediately frozen at–20°C. Within up to 3 days, samples were thawed, diluted with 1:3 phosphate-buffered saline solution, and homogenized. Aliquots were stored in a 2 mL microcentrifuge safe-lock tub at –80°C. Frozen aliquoted fecal samples (–80°C) from stool homogenization were used for shotgun metagenomics sequencing in the current study. The original study included up to 10 stool samples from each patient, but the current secondary analysis included one sample from each participant within the week two timeframe of inpatient treatment in which the sample closest to the date of the structural MRI was reprocessed for shotgun sequencing (approximately days 8–14 of inpatient treatment).

### Fecal shotgun metagenomics sample processing methods

DNA was extracted from approximately 50 mg of stool samples in two stages including an initial homogenization in Lysis Matrix E tubes (MP Biomedicals) with a Precellys 24 Tissue Homogenizer (Bertin Instruments) and subsequent processing of the resultant supernatant using the MagAttract PowerMicrobiome DNA/RNA EP kit (Qiagen) on an Eppendorf automated liquid handling system as per the manufacturer's instructions. Isolated DNA was then checked for concentration and quality on a BioTek Synergy HTX plate reader. Metagenomic libraries were prepared using the Nextera DNA Flex

Library Prep Kit (Illumina) per the manufacturer's instructions with 100 ng of DNA as sample input. The concentration of the resultant libraries was quantified using the Qubit dsDNA HS assay on a Qubit 2.0 fluorometer (Life Technologies). Library size and quality were assessed via the Agilent High Sensitivity D5000 ScreenTape on an Agilent 4200 Tapestation. Metagenomic libraries were normalized to an equimolar concentration and pooled. The pool was diluted to 1.8 PM, mixed with a 1% PhiX control library, and sequenced via a pairedend run (75 bp×75 bp) using a NextSeq 500/550 High Output v2 150-cycle Reagent Cartridge on a NextSeq 500 sequencer (Illumina).

#### Shotgun metagenomics bioinformatics processing

#### FASTQ file processing

This work utilized the computational resources of the NIH HPC Biowulf cluster (http://hpc.nih.gov). A total of 16 paired-end raw FASTQ files were submitted for quality control and processing. Shotgun sequencing analysis was conducted using the 'Just a Microbiology System' 1.7.9 (JAMS) package which can be found on GitHub (https://github.com/johnmcculloch/JAMS BW) (McCulloch et al., 2023). All FASTQ files were submitted to FastQC (v0.11.9, https://www.bioinformatics.babraham.ac.uk/projects/fastqc/) for quality control checking and further submitted for quality trimming using Trimmomatic v0.36 (Bolger et al., 2014) with the following parameters: leading=15, trailing=15, slidingwindow=4:18, headcrop=0, minlen=36. Shotgun metagenomics sequence reads were aligned against the human genome (human genome build: GRCh38. p14) with Bowtie2 v2.3.2 (Langmead & Salzberg, 2012) to remove host contamination. All unaligned reads were then assembled using MEGAHIT v1.2.9 (Li et al., 2015) within the JAMSalpha package.

#### Microbiome characterization

Taxonomy classification of the contigs was carried out using Kraken2 (Wood et al., 2019) in JAMSalpha, and only contigs greater than 500 base pairs were considered for taxonomic classification. A custom 90 Gigabyte Kraken2 database was built January 2022 in JAMS from draft and complete genomes of all bacteria, archaea, fungi, viruses, and protozoa available in the NCBI GenBank (as of January 2022) using the JAMSbuildk2db tool of the JAMS package (database name/version: JAMSdb202201\_1.6.6\_20220114). Taxonomy was expressed as the last known taxon (LKT), i.e., the classification with the lowest unambiguous taxonomic level. Alpha diversity indices (Inverse Simpson, Shannon Diversity Index, and Chao1) were computed on the LKT parts per million (PPM) count table generated using the minimal filtering setting in JAMSbeta v1.8.3, which required genome completeness to be at least 5% in at least 5% of samples (McCulloch et al., 2023). Higher-order taxonomic summaries were calculated by collapsing the remaining LKT features after the minimal filtering setting at the levels of phylum and genus, respectively.

29937175, 2024, 7, Downloaded from https://onlinelibrary.wiley.com/doi/10.1111/acer.15346 by Nat Prov Indonesia, Wiley Online Library on [16/07/2024]. See the Terms

and-conditions) on Wiley Online Library for rules

of use; OA

articles are governed by the applicable Creative Commons

#### Abundance filtering and transformation

The top 100 most counted or "highly abundant" taxa were selected for downstream microbiome-associated bivariate analyses. The minimal filtering setting in JAMSbeta v1.8.3, i.e., genome completeness required to be at least 5% in at least 5% of samples, was also used to generate the bacterial feature table, and the 100 LKT with the greatest average part per million counts were extracted as the highly abundant taxa. The centered log ratio with parameterization (CLRp) transformation was computed on the highly abundant LKT feature table to account for compositionality and allow for downstream parametric testing (Erb, 2023). Scripts to perform CLRp transformation are publicly available for download from GitHub (https://github.com/thomazbastiaanssen/deleuze).

#### Gut-Brain module analysis workflow

To support the clinical interpretation of microbiome-associated feature data, GBMs were computed from metagenomic sequencing data. GBMs represent functional pathways curated from the literature that have been reported to take place in the gut microbiome and are involved in microbiome-gut-brain communication (Valles-Colomer et al., 2019). Each GBM corresponds to a single neuroactive compound production or degradation process. To compute GBMs, bacterial functional potential identifiers were obtained using the NIH Nephele platform from the National Institute of Allergy and Infectious Diseases Office of Cyber Infrastructure and Computational Biology, a microbiome analysis cloud-based platform for whole genome sequencing (https://nephele.niaid.nih. gov) (Weber et al., 2018). Specifically, the whole genome sequencing bioBakery workflow (Beghini et al., 2021) was run on Nephele to construct a gene function relative abundance table output from HUMAnN v3.0.0.alpha.3 (Franzosa et al., 2018). From this gene function relative abundance table, the genefamilies relab.tsv file was converted to Kyoto Encyclopedia of Genes and Genomes (KEGG) ids using the following command: humann regroup table with the -g flag as uniref90\_ko. The KEGG id abundance table was then split using the humann\_split\_stratified\_table command within HUMAnN to be used in the GBM workflow. KEGG pathways used to build GBMs were downloaded from https://raeslab.org/software/gbms. html. The KEGG relative abundance feature table data was mapped to GBMs using Omixer-rpmR; a reference pathway mapping tool for metabolic module profiling of microbiome samples modified for the R programming environment (https://github.com/omixer/omixe r-rpmR). The CLRp transformation was also performed on the GBM feature table for downstream statistical analysis.

#### Statistical analyses

All statistical analyses were conducted using  $JMP^{TM}$  v16.0 (SAS Headquarters, Cary, NC) and the R programming environment.

Means and standard deviations were calculated to describe group values of features across the study cohort. Because of the small and heterogenous sample, along with the exploratory nature of this work, bivariate comparisons were performed using Pearson correlations between alcohol-associated clinical symptom severity and brain ROI morphometry, microbiome-associated features and brain ROI morphometry, and microbiome-associated features and alcoholassociated clinical symptom severity, respectively (Figure 1B). Alcohol-associated clinical symptoms that were used in bivariate analyses included withdrawal from alcohol, sleep quality, depression, anxiety, and craving for alcohol. Bivariate relationships between GBMs and the top 100 most abundant gut microbiome taxa were also calculated to identify taxa-GBM correlation pairs. Descriptive statistics are presented for other relevant demographic information, clinical and nutrition data, drinking patterns, and alcohol dependence severity data representing the study cohort in Table 1.

Multiple comparisons correction was applied to statistical comparisons using the Benjamini–Hochberg post hoc procedure (False Discovery Rate [FDR]) when testing associations between brain ROIs and clinical symptom severity, brain ROIs and microbiome features, and microbiome features and clinical symptom severity, respectively. As this is an exploratory study intended to produce preliminary data for future hypotheses, a q-value of 0.2 (i.e., an FDR corrected p-value <20%) was used as a threshold for statistical significance in the FDR corrected p values. Data are expressed as mean  $\pm$  standard deviation.

#### **RESULTS**

### Clinical, MRI, and microbiome characteristics of study population

A total of 16 participants had structural MRI, gut microbiome samples, and clinical phenotype data, and therefore were included in this secondary analysis study. Participants were  $45\pm11.6$  years of age with a BMI of  $23.89\pm2.48$  and were mostly white (56.25%) males (62.5%) who were current smokers (62.5%; see Table 1A for demographic and clinical averages of the study cohort). Participants reported an average of  $18.44\pm12.12$  heavy drinking years and an average of  $17.16\pm9.78$  drinks per day in the 90 days preceding inpatient admission. The HEI for this inpatient cohort was  $61.96\pm10.52$ , and the total dietary fiber intake was  $27.28\pm13.70$  g.

Mean values of brain ROI for volume (normalized to total brain volume without ventricles), surface area (normalized to white matter surface area), and cortical thickness values are shown in Table 1B. The mean gut microbiome sequencing depth was  $4.44\pm0.53$  Gigabase pairs before trimming, and  $4.16\pm0.50$  Gigabase pairs after trimming, yielding an average assembly rate of  $87.4\pm5.1\%$  (see Table S2 for all FASTQ read statistics). A total of 9705 taxa were annotated in the gut microbiome samples after filtering in JAMS. The average Shannon diversity index of the patient cohort was  $3.67\pm0.40$  (see Figure S1 for all alpha diversity metrics calculated), and across







A. Demographics, clinical characteristics, and alcohol intake profiles								
Characteristic, n = 16	Mean ± SD or N (%)							
Age (years)	45 ± 11.61							
ВМІ	$23.87 \pm 2.47$							
Sex								
Male	10 (62.5%)							
Female	6 (37.5%)							
Race								
White (non-Hispanic)	9 (56.25%)							
Black (non-Hispanic)	5 (31.25%)							
Black (Indigenous/non-Hispanic)	1 (6.25%)							
Unknown Hispanics	1 (6.25%)							
Smoking status								
Smoker	10 (62.5%)							
Non-smoker	5 (31.25%)							
Missing	1 (6.25%)							
	Mean <u>+</u> SD							
ВМІ	$23.89 \pm 2.48$							
	N (%)							
Mood disorder								
Yes	5 (31.25%)							
Anxiety disorder								
Yes	5 (31.25%)							
	Mean ± SD							
Subjective symptoms								
BSA	$6.56 \pm 5.05$							
MADRS	$8.13 \pm 4.38$							
PSQI Global Score	12.21±3.89							
CIWA <sup>a</sup>	$5.81 \pm 2.93$							
PACS	$10.31 \pm 7.28$							
Bristol Stool Scale	3.75 ± 1.39							
Drinking measures								
Average drinks per day	$17.16 \pm 9.78$							
Number of heavy drinking days	$76.40 \pm 22.77$							
Number of heavy drinking years	$18.44 \pm 12.12$							
ADS Score	$21.60 \pm 4.21$							
AUDIT total	$30.27 \pm 4.85$							
OCDS total	19.60 ± 9.45							
Nutrition	(4.0/_40.50							
Total HEI-2015	61.96±10.52							
Energy (kcal)	2622.28±982.08							
Total carbohydrate (g)	316.94±128.99							
Total protein (g)	120.64±30.52							
Total fat (g)	102.48 ± 55.47							

TABLE 1 (Continued)

A. Demographics, clinical characteristics, and alcohol intake profiles										
Characteristic	Mean ± SD or N (%)									
Total dietary fiber (g) $27.28 \pm 13.70$										
B. Morphometry of brain regions of interest from structural MRI										
Brain region of interest (n = 16)	Volume Surface area (normalized %)		Cortical thickness (mm)							
ACC	$0.752 \pm 0.104$	3.451±0.464	$2.522 \pm 0.176$							
Amygdala	$0.288 \pm 0.027$	N/A	N/A							
Hippocampus	$0.735 \pm 0.080$	N/A	N/A							
Insula	1.200±0.082	$2.879 \pm 0.114$	$2.879 \pm 0.114$							

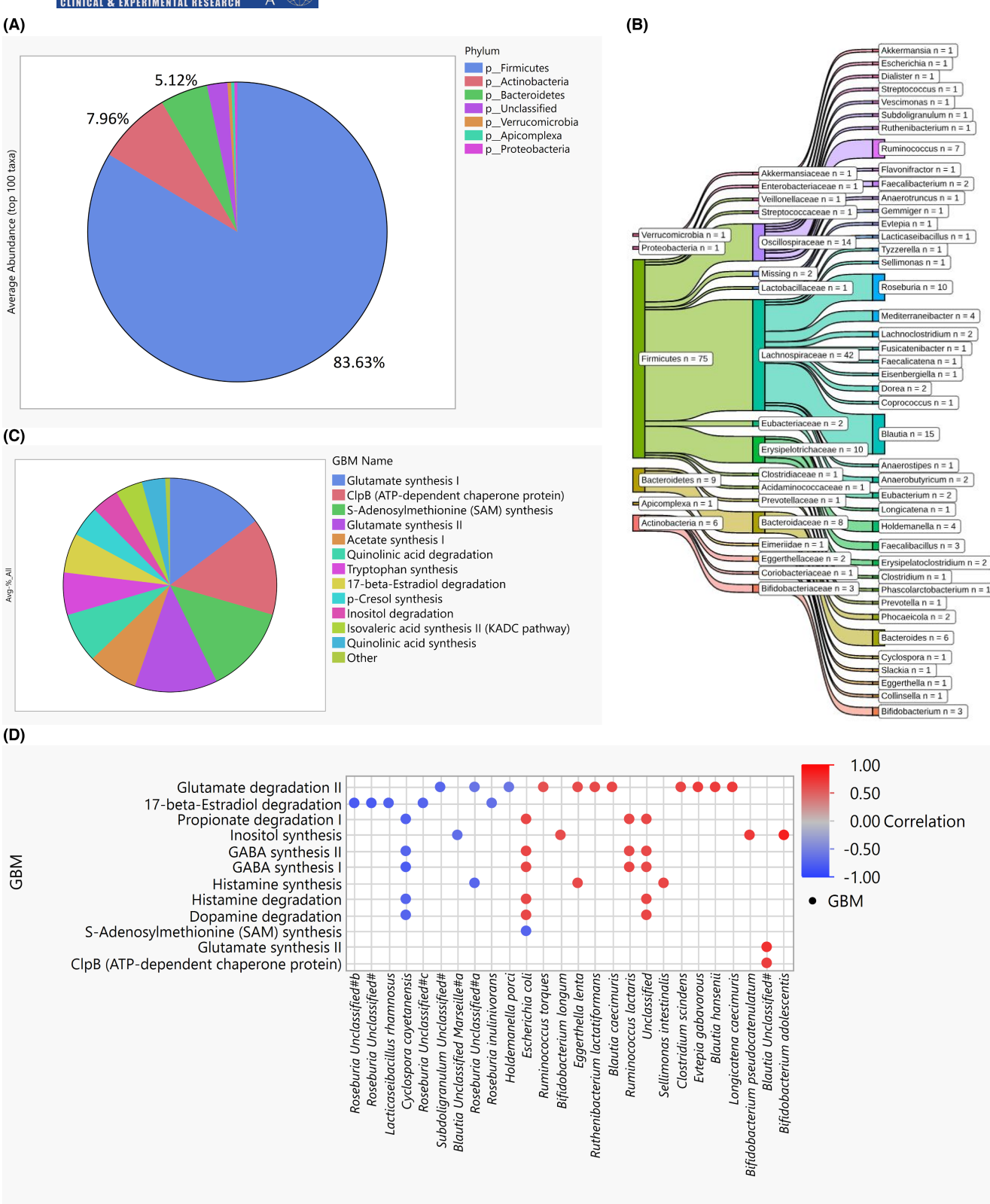
Note: (A) Demographics, clinical characteristics, symptom, and alcohol intake data in the study cohort. <sup>a</sup>Maximum CIWA score over the first 4 days at the start of treatment. (B) Volume, surface area, and cortical thickness values of brain regions of interest in the study cohort. Normalized volume measures were calculated by dividing each regional volume measure by the brain volume (without ventricles), and normalized surface area measures were calculated by dividing the surface area of each bilateral composite region with the white matter surface area in each hemisphere.

Abbreviations: ACC, anterior cingulate cortex; ADS, Alcohol Dependence Scale; AUDIT, Alcohol Use Disorders Identification Test; BMI, body mass index; BSA, Brief Scale for Anxiety; CIWA, Clinical Institute Withdrawal Assessment; HEI, Health Eating Index; kcal, kilocalorie; MADRS, Montgomery Asberg Depression Rating Scale; OCDS, Obsessive Compulsive Drinking Scale; PACS, Penn Alcohol Craving Scale; PSQI, Pittsburg Sleep Quality Index.

all 9705 taxa, Firmicutes predominated gut microbiome samples  $(81.72 \pm 11.68\%)$ , followed by Actinobacteria  $(8.32 \pm 10.51\%)$  and Bacteroidetes ( $5.43 \pm 6.75\%$ ). This distribution at the phylum level was similar when the top 100 most abundant taxa (used for downstream analysis) were averaged, with Firmicutes 83.63 ± 11.72%, Actinobacteria ( $7.96 \pm 10.53\%$ ) and Bacteroidetes ( $5.12 \pm 6.71\%$ ) encompassing the most abundant phyla (Figure 2A). The greatest number of the abundant genera originated from the Lachnospiraceae family (n=42), and the taxonomic lineage of the top 100 genera is illustrated in Figure 2B. Of these genera, Blautia had the highest relative abundance (26.15 ± 8.61%), followed by Ruminococcus  $(11.22 \pm 9.47\%)$  and Roseburia  $(6.03 \pm 5.96\%)$ ; Figure S2). Notably, there was a large degree of variation across individual participants in the PPM abundance quantified of these top 100 taxa (Figure S3).

A total of 4489 KEGG orthologs were extracted from the bio-Bakery HUMAnN3 functional analysis, and 38 GBMs were detected after running the GBM workflow (Figure S4). The top 4 most abundant GBMs were the ClpB (ATP-dependent chaperone protein), Glutamate synthesis I, S-Adenosylmethionine (SAM) synthesis, and Glutamate synthesis II pathways with 12.42%, 12.22%, 11.65%, and 10.44% average abundance (of total GBMs identified), respectively (Figure 2C). When each GBM was correlated with the top 100 taxa, there were 44 significant GBM-taxa pairs that consisted of 25

29937175, 2024, 7, Downloaded from https://onlinelibrary.wiely.com/doi/10.1111/acer.15346 by Nat Prov Indonesia, Wiley Online Library on [16/07/2024]. See the Terms and Conditions (https://onlinelibrary.wiely.com/rems-and-conditions) on Wiley Online Library for rules of use; OA articles as governed by the applicable Creative Commons License



Taxa

FIGURE 2 Gut microbiome community characteristics of study cohort. (A) Average relative abundance of the top 100 most abundant gut microbiome taxa at the phylum level. (B) Sankey diagram displaying the composition and lineage at the phylum, family, and genus level for the top 100 taxa with the total count at each level. (C) Average representation of GBMs identified (% of total) from gut microbiome samples. (D) Pearson correlation coefficient (r) dot plot representing relationships between GBMs and the top 100 taxa in gut microbiome samples. Before FDR correction, a total of 261 pairs of taxa and GBM associations were found to be significant, which consisted of 76 unique taxa and 38 GBMs (Table S3). Several *Roseburia* species were negatively associated with 17-beta-Estradiol degradation, while the Glutamate degradation II pathway was positively associated with multiple taxa including two *Blautia* species (*Blautia caecimuris* and *Blautia hansenii*). GBM-taxa pair associations shown are those that were significant at *q* < .20 after FDR correction (representing 25 unique taxa and 12 unique GBMs). Heatmap indicates correlation coefficient. *Blautia Unclassified* # = *Blautia Unclassified MSJ* 36, *Blautia Unclassified Marseille* # = *Blautia Unclassified Marseille* P3201T, *Roseburia Unclassified* # = *Roseburia Unclassified* CLA AA H209, *Roseburia Unclassified* CLA AA H204, *Subdoligranulum Unclassified* # = *Subdoligranulum Unclassified* APC924 74.

TABLE 2 Brain region of interest and clinical symptom correlations.

	Withdrawal			Anxiety		Depression		Craving for alcohol			Sleep quality				
Brain ROI	r	р	q	r	р	9	r	р	9	r	р	q	r	р	q
Volume															
ACC	0.13	0.63	0.72	-0.39	0.14	0.45	-0.28	0.30	0.79	-0.21	0.43	0.69	0.23	0.44	0.88
Amygdala	0.32	0.22	0.35	-0.04	0.88	0.95	0.12	0.67	0.83	-0.45	0.08	0.67	0.04	0.88	0.88
Hippocampus	-0.10	0.73	0.73	-0.18	0.52	0.90	0.07	0.81	0.83	-0.27	0.30	0.69	0.40	0.16	0.74
Insula	0.34	0.20	0.35	-0.09	0.75	0.95	-0.21	0.44	0.83	-0.32	0.23	0.69	-0.21	0.48	0.88
Surface area															
ACC	0.36	0.17	0.35	-0.02	0.95	0.95	0.11	0.67	0.83	-0.14	0.62	0.79	0.38	0.18	0.74
Insula	0.60	0.01*	0.11	0.16	0.56	0.90	-0.06	0.83	0.83	-0.07	0.79	0.79	0.09	0.76	0.88
Cortical thickness															
ACC	-0.41	0.11	0.35	-0.46	0.07	0.45	-0.48	0.06	0.48	0.24	0.37	0.69	-0.06	0.83	0.88
Insula	-0.30	0.27	0.36	-0.36	0.17	0.45	-0.35	0.18	0.73	0.07	0.79	0.79	-0.06	0.76	0.88

*Note*: Withdrawal was evaluated by the average of the max CIWA scores for days 1–4 of treatment, Anxiety was evaluated using the BSA, Depression was evaluated using the MADRS, Craving was evaluated using the PACS, and sleep quality was evaluated using the PSQI. Pearson correlation coefficients (r) reported. \*p < 0.05, \*\*q < 0.05.

Abbreviation: ACC, anterior cingulate cortex.

unique taxa and 12 unique GBMs (Figure 2D). See Table S3 for the results of all bacterial and GBM correlations performed.

## Clinical phenotype relationships with brain morphometry and microbiome-associated features

Brain morphometry regions were correlated with clinical symptom phenotypes, and insula surface area was positively associated with alcohol withdrawal severity scores (r=0.60, q=0.107; Table 2; Figures S5 and S6H). Cortical thickness of the ACC was moderately negatively associated with both depression (r=-0.48, q=0.485, Figure S7C) and anxiety (r=-0.46, q=0.449; Figure S7F), but neither reached statistical significance. Amygdala and hippocampus morphometry were not associated with clinical symptom severity in this study cohort (Figure S5, Table S4).

Clinical symptom scores were correlated with alpha diversity metrics to investigate any associations in overall gut microbial

diversity with clinical phenotypes of patients with AUD and none were significantly correlated (Figure 3A, Table S5). When individual taxa were assessed with clinical phenotypes, there were 18 taxa that had moderate associations with alcohol-associated clinical symptoms that were significant before FDR correction (p < 0.05), including five classified to the genus Blautia, but Blautia hansenii abundance and subjective depression severity was the only relationship that was statistically significant after multiple comparisons correction (r=0.74, q=0.099; Figure 3B, Table S3). When GBM pathway relative abundance was correlated against clinical symptom severity, the abundance of several GBM pathways was positively associated with anxiety (Figure 3C). GBM pathways positively correlated with anxiety severity included Dopamine degradation (r=0.54, q=0.218), GABA synthesis I and II (r=0.54, q=0.218; r=0.53, q=0.218, respectively), Histamine degradation (r=0.54, q=0.218), Propionate degradation I (r=0.54, q=0.218), and Nitric oxide degradation I (r=0.49, q=0.271), however, none of these correlations were statistically significant (Table S3).

29937175, 2024, 7, Downloaded from https://onlinelibrary.wiley.com/doi/10.1111/acer.15346 by Nat Prov Indonesia, Wiley Online Library on [16/07/2024]. See the Terms and Conditions (https://onlinelibrary.wiley.com/wems/

and-conditions) on Wiley Online Library for rules of use; OA articles are governed by the applicable Creative Commons License

#### Brain morphometry and microbiome comparisons: Amygdala volume associated with multiple gut microbiome biomarkers

When morphometry of brain ROIs and alpha diversity metrics (i.e., Shannon Index, Inverse Simpson, and Chao1) were compared, amygdala volume was positively associated with Shannon Index (r=0.53, q=0.147; Figure 4A, Figure S8A), while ACC cortical thickness was negatively associated with Shannon Index (r=-0.53, q=0.147; Figure 4A, Figure S8B). Similar relationships were observed between Chao1 and both ACC cortical thickness and amygdala volume (r=-0.47, q=0.274; r=0.49, q=0.274, respectively), but

these relationships did not reach statistical significance (Figure 4A, Table S6). Of the brain morphometric values correlated with the relative abundance of individual taxa, the amygdala was the sole ROI that had statistically significant associations (Figure 4B, Table S3). The bacterial taxa significantly correlated with amygdala volume included negative associations with Anaerostipes hadrus (r=-0.64, q=0.123), Dorea formicigenerans (r=-0.66, q=0.105), Blautia obeum (r=-0.67, q=0.105), Blautia (r=-0.58, q=0.176), Ruminococcus (r=-0.72, q=0.058), and Eubacteriales (r=-0.60, q=0.168), and positive associations with Bacteroides uniformis (r=0.72, q=0.058), Phocaeicola dorei (r=0.61, q=0.168), Phocaeicola vulgatus (r=0.72, q=0.058), and Bacteroidaceae (r=0.57, q=0.198). GBMs also were

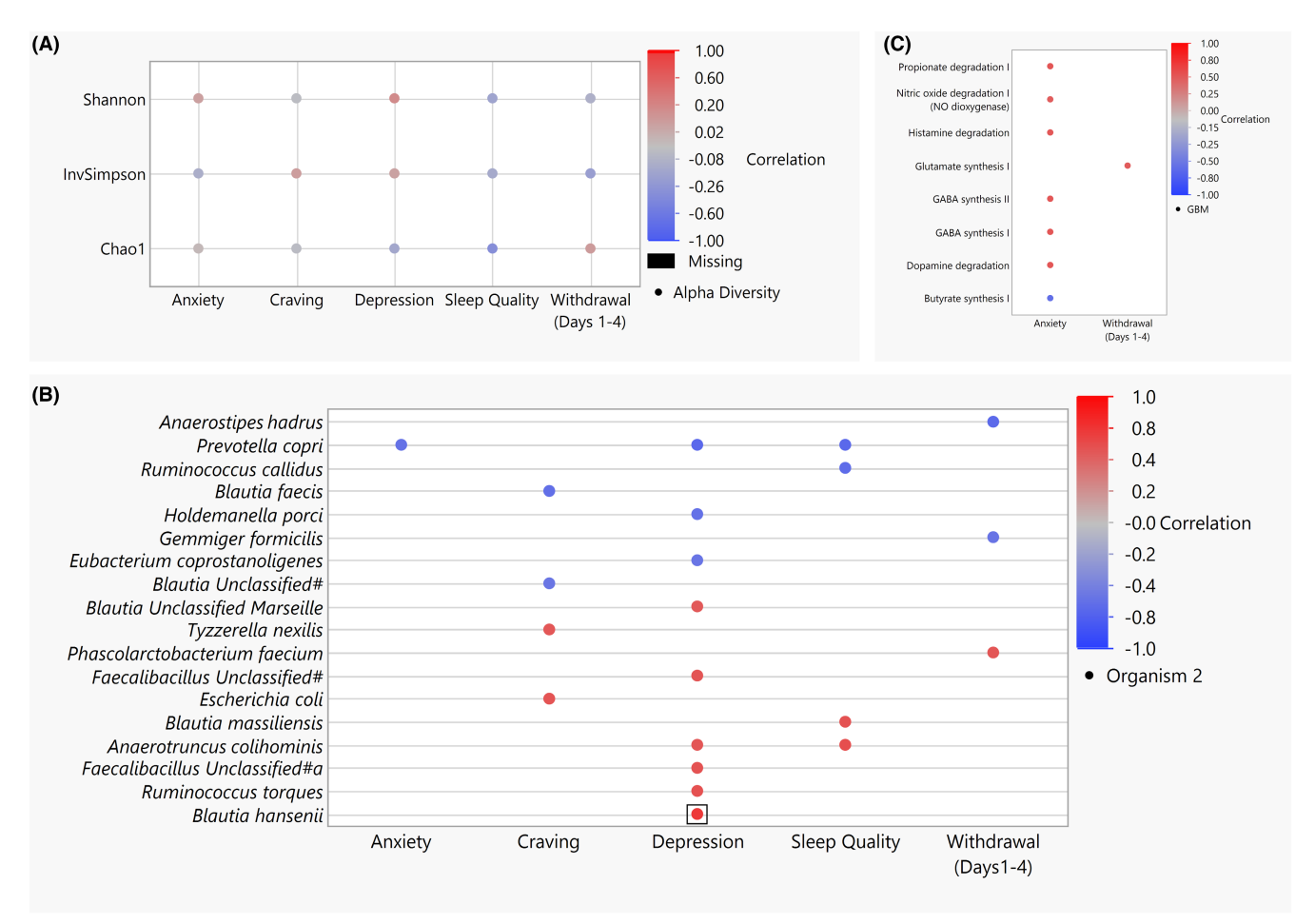
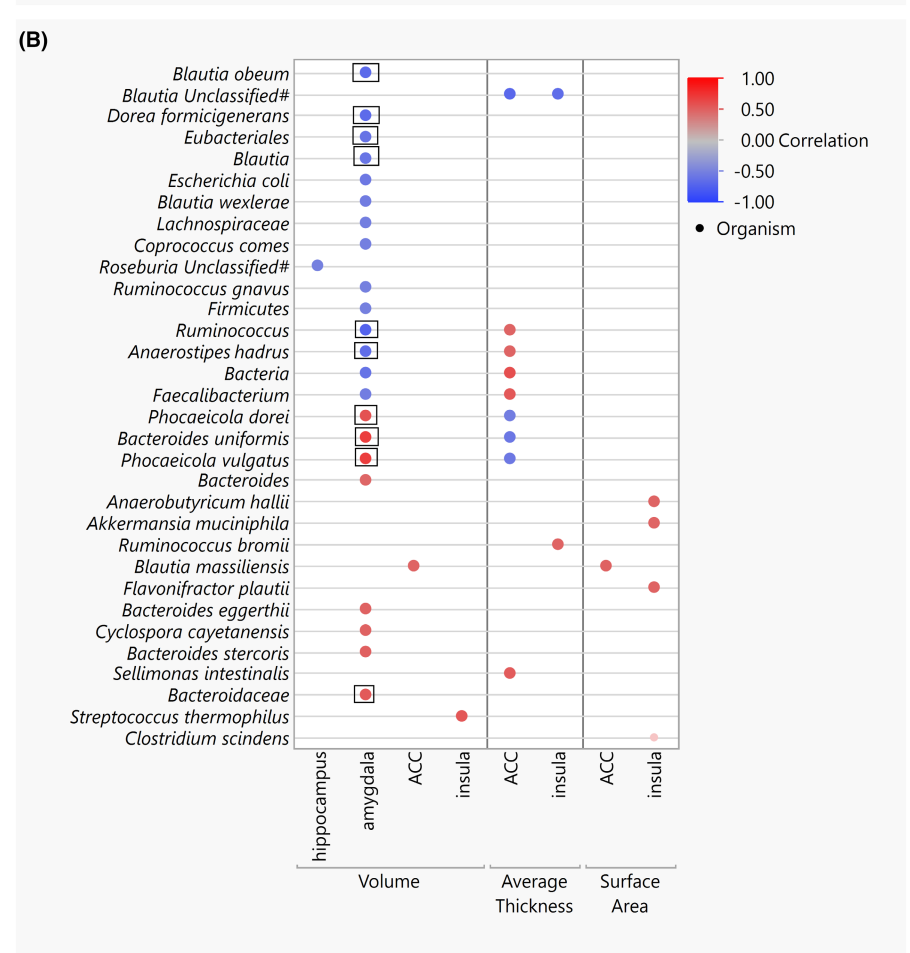
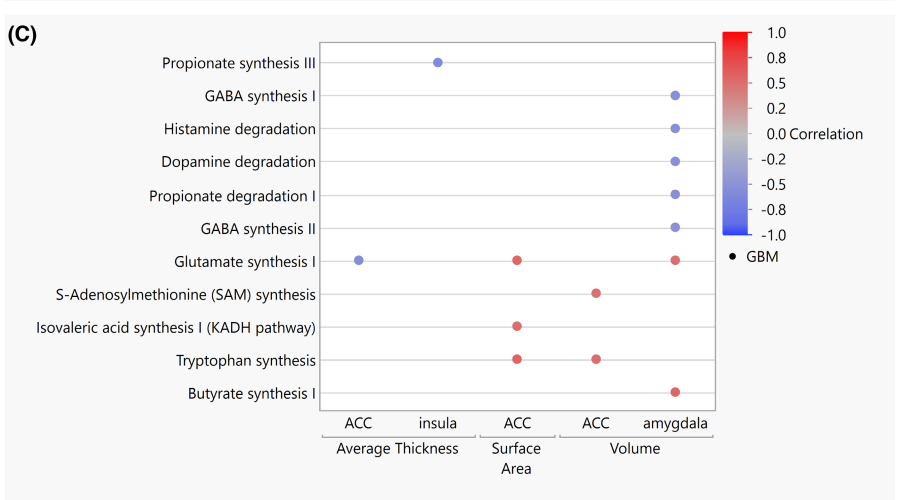


FIGURE 3 Gut microbiome taxonomic and functional associations with clinical phenotype. (A) Pearson correlation coefficient (r) dot plot of alpha diversity metrics with clinical symptom scores. (B) Pearson correlation coefficient (r) dot plot of bacterial taxa abundance with clinical symptom scores. Blautia Unclassified # = Blautia Unclassified MSJ, Faecalibacillus Unclassified # = Faecalibacillus Unclassified H12, Faecalibacillus Unclassified # = Faecalibacillus Unclassified MSK20. (C) Pearson correlation coefficient (r) dot plot of GBM pathway abundance with clinical symptom scores. For all plots, the heatmap indicates the correlation coefficient. All dots on the plot represent unadjusted p < 0.05, except for panel A where all comparisons are shown. Boxes indicate statistical significance of FDR q < 0.20.

FIGURE 4 Gut Microbiome Taxonomic and Functional Associations with Brain ROIs. ACC, anterior cingulate cortex; InvSimpson, Inverse Simpson. (A) Pearson correlation coefficient (r) dot plot of alpha diversity metrics with brain ROIs. (B) Pearson correlation coefficient (r) dot plot of taxa abundance with brain ROIs. Blautia Unclassified = Blautia Unclassified DFI 4 84, Roseburia Unclassified = Roseburia Unclassified CLA AA H204. (C) Pearson correlation coefficient (r) dot plot of GBM pathway abundance with brain ROIs. For all plots, the heatmap indicates the correlation coefficient. All dots on the plot represent unadjusted p < 0.05, except for panel A where all comparisons are shown. Boxes indicate statistical significance of FDR q < 0.20.





correlated with brain ROI measures and a similar predominance of amygdala morphometry associations occurred, with seven GBM pathways demonstrating moderate GBM-amygdala volume associations (Figure 4C). Although not statistically significant, positive associations between GBMs and amygdala volume were seen with the Butyrate synthesis I (r=0.57, q=0.247) and Glutamate synthesis I (r=0.51, q=0.247) pathways, while negative GBM associations with amygdala volume included Dopamine degradation (r=-0.53, q=0.247), GABA synthesis II (r=-0.51, q=0.247), Histamine degradation (r=-0.53, q=0.247), and Propionate degradation I (r=-0.53, q=0.247; Table S3).

#### DISCUSSION

AUD is an incredibly complex disorder with neurologic (Carbia et al., 2021; Koob & Colrain, 2020) and gastrointestinal (Bishehsari et al., 2017) pathology, which provides a multitude of potential gutbrain signaling pathways. Shared withdrawal, sleep disturbance, craving, anxiety, and depressive symptoms that are frequently experienced by patients with AUD during detoxification from alcohol impact both treatment efficacy and risk for relapse (Ames et al., 2020; Wallen et al., 2019). Although this exploratory research can only provide preliminary evidence of possible gut-brain signaling mechanisms in AUD, we discovered clinically and statistically significant microbiome-associated features that had shared associations with brain morphometry and clinical symptoms that can be used to inform future hypothesis-driven prospective research.

### Amygdala volume is associated with several microbial features in patients with AUD

The amygdala had the strongest and most consistent relationships with the gut microbiome in this study, having significant associations with the abundance of several taxa in addition to gut microbiome community measures (i.e., alpha diversity). We were specifically interested in amygdala volume as a brain ROI in this research due to previous morphometric variation associations with heavy alcohol use, AUD, and stress-associated disorders (Lautarescu et al., 2020; Senatorov et al., 2015). Amygdala volume was positively correlated with alpha diversity metrics of microbial richness (Chao 1) and both richness and evenness (Shannon index), although Chao1 associations with amygdala volume did not meet statistical significance (p=0.052). Ten taxa were significantly positively and negatively associated with amygdala volume. The positively associated taxa with amygdala volume fell under the Bacteroidaceae family, while the negatively associated taxa (Dorea formicigenerans, Blautia obeum, and LKT Blautia) were classified to the same genera previously implicated with increased intestinal permeability in individuals with AUD (Leclercq, Matamoros, et al., 2014). Increased intestinal permeability facilitates translocation of bacterial byproducts (such as endotoxin) into the systemic circulation (Bishehsari et al., 2017; Leclercq et al., 2012), and has been shown to be associated with elevated markers of inflammation and end-organ disease in patients with AUD, irrespective of the amount of alcohol consumed prior to inpatient treatment (Leclercq, Matamoros, et al., 2014).

Several GBMs were also found to be significantly associated with amygdala volume, such as negative associations with GABA synthesis pathways and positive associations with glutamate synthesis pathways, which are involved with the modulation of excitatory signaling involved in symptoms such as withdrawal and anxiety. These associations suggest that microbiome-associated signaling pathology to the amygdala may involve a disruption in the balance of functional genes involving inhibitory and excitatory neurotransmitter signaling pathways. Whether or not the increase or decrease in the components of these GBM pathways in fecal samples leads to a measurable change in gut-brain signaling, or if the increase or decrease in GBM abundance is a cause or a compensatory mechanism from the pathology leading to increased symptom severity is not known at this time. Continued research with larger sample sizes in patients with and without AUD will build on these preliminary findings.

Nevertheless, there is well-described research linking the structure, function, and development of the amygdala to the gut microbiome in rodent and human studies. In germ-free mice lacking a gut microbiome, several altered characteristics of the amygdala have been reported including lower BDNF expression, higher volumes, and hyperactivity of neuronal systems including synaptic and cholinergic transmission (Hoban et al., 2018; Stilling et al., 2015). In humans, probiotic supplementation with Bifidobacterium longum NCC3001 reduced both amygdala-associated negative emotional stimuli responses and subjective depression scores in subjects with irritable bowel disease (Pinto-Sanchez et al., 2017). Therefore, our findings contribute to the accumulating evidence supporting gutbrain signaling pathways from the gut microbiome to the amygdala and provide early evidence of potential taxa-specific associations that may be investigated in future research of mechanisms underlying microbiome-associated neuropathology in AUD.

# Disparate brain and clinical feature associations with *Blautia* species suggest heterogeneous functions of *Blautia*-associated taxa

Several *Blautia* taxa were associated with brain ROI morphometry, clinical symptom severity, and clinically relevant GBM pathways in this population of treatment-seeking subjects with AUD. For example, in addition to the previously described relationships between *Blautia* taxa and amygdala volume, *Blautia Unclassified DFI 4 84* was negatively associated with both ACC and insular cortical thickness. The abundance of *Blautia massiliensis* was positively associated with both ACC volume and surface area, along with reductions in subjective sleep quality (as indicated by an increased PSQI score). Subjective reports of increased symptoms of depression were positively associated with *Blautia hansenii* and *Blautia Unclassified Marseille P3201T* abundance while craving scores were negatively



associated with Blautia faecis and Blautia Unclassified MSJ 36. It is important to note that not all reported associations remained significant after FDR correction, but these shared relationships between Blautia taxa, brain morphometry, symptom measures, and functional microbiome data (i.e., GBMs) provide important preliminary information supporting further discovery.

In the literature, Blautia taxa have been hypothesized to have multiple roles and relationships with human physiology, ranging from metabolic properties beneficial for human health to association with clinical markers of disease (Leclercq et al., 2021; Leclercq, Matamoros, et al., 2014; Liu et al., 2021). Research annotating Blautia at the taxonomic level of genus and species has reported both positive and negative associations with sleep quality across measures of sleep efficiency, total sleep time, and subjective sleep quality (Smith et al., 2019). The connection of Blautia taxa to sleep in the literature supports our finding connecting Blautia massiliensis abundance to poor subjective sleep quality. As most currently available research has been performed using genus-level taxa, future work with species-level data will clarify if the divergent relationships of sleep quality with Blautia taxa are species-specific or more dependent on patient phenotype and environmental conditions. Blautia abundance has also been connected to heavy alcohol use and known complications of AUD in other research. For example, a recent binge drinking episode was associated with an increase in the abundance of Blautia wexlerae (Carbia et al., 2023), and the relative abundance of Blautia was positively associated with markers of intestinal permeability linked to increased inflammation and systemic complications (Leclercy, Matamoros, et al., 2014).

In microbiome niches such as the gut microbiome, different Blautia species may metabolize heterogenous metabolites or other mediators that signal to the brain in a manner that differentially impacts subjective anxiety, depression, sleep disruption, or craving depending on the environmental conditions and substrates. For example, until the isolation and classification of gram-negative Blautia massiliensis, the entirety of the genus Blautia was thought to be gram positive prompting a revised description of the genus (Durand et al., 2017). Several Blautia species including Blautia massiliensis (associated with poor sleep quality) were positively associated with an increased abundance of the tryptophan synthesis pathway. Other Blautia species had incongruent associations with GBM pathways. For example, Blautia hansenii was positively associated with quinolinic acid degradation, while Blautia Unclassified MSJ 36 was negatively associated with quinolinic acid degradation. Quinolinic acid, a neurotoxic byproduct of the kynurenine pathway associated with glutamate release and reactive oxygen species, is significantly elevated in treatment-seeking patients with AUD (Leclercq et al., 2021). We report positive associations between amygdala volume and ACC surface area with glutamate synthesis I in our patient cohort, suggesting a potential relationship between Blautia species and byproducts of the kynurenine pathway that can be explored in future research. Importantly, the specific role of different Blautia species in human health and

AUD-associated disease remains to be determined in future confirmatory and mechanistic research.

#### Additional putative gut-brain signaling associated bacteria: Phocaeicola dorei, Phocaeicola vulgatus, Escherichia coli, Prevotella copri, and Ruminococcus

Other bacteria that were relevant in this analysis due to collective associations across clinical phenotype, brain ROI, and GBM domains included Phocaeicola dorei, Phocaeicola vulgatus, Escherichia coli, Prevotella copri, and Ruminococcus taxa. The abundance of Phocaeicola dorei and Phocaeicola vulgatus taxa were both negatively associated with ACC average thickness and positively associated with the GBM pathway glutamate synthesis I. Increased glutamate synthesis in gut microbiome communities shows relevance for alcohol-specific symptoms. For example, in our research, higher withdrawal scores were associated with increased glutamate synthesis, while another study reported associations between increased fecal GBM glutamate synthesis pathways and higher craving scores in young adult binge drinkers (Carbia et al., 2023). Phocaeicola dorei and Phocaeicola vulgatus may have possible roles in bile acid deconjugation, as levels of these taxa have been correlated with unconjugated bile acids in fecal microbiome transplant studies and have been shown to produce bile salt hydrolase using in vitro experiments (Bustamante et al., 2022; Xu et al., 2023). These bacteria have been linked to the production of short-chain fatty acids (Ó Cuív et al., 2017), and we observed moderate positive associations between Phocaeicola vulgatus and the butyrate synthesis I pathway, and negative associations occurred between Phocaeicola dorei and propionate Degradation I. Increased bile acid excretion and short chain fatty acid synthesis are considered positive gut-brain signaling mechanisms through a reduction of inflammation (Xu et al., 2023), parasympathetic nervous system activation (Cryan et al., 2019), and modulation of microglia function (Erny et al., 2015). Therefore, further investigation into the directionality and clinical implications of physiologic Phocaeicola taxa associations, such as increased bile acid excretion and short-chain fatty acid synthesis, versus pathologic pathways like increased glutamate synthesis may inform the role of these taxa in brain signaling and the associated mechanisms.

The abundance of Escherichia coli in gut microbiome samples was associated with brain ROI morphometry, clinical symptom severity, and GBM abundance in our study cohort. Escherichia coli was negatively associated with amygdala volume and was positively associated with craving for alcohol. Escherichia coli also had significant associations with several GBM pathways including a positive association with dopamine degradation, histamine degradation, GABA synthesis I and II, and propionate degradation I, and a negative association with S-Adenosylmethionine (SAM) synthesis. Shared negative associations between amygdala volume and both Escherichia coli and S-Adenosylmethionine (SAM) synthesis, along with the known associations of Escherichia coli to mechanisms

involving inflammation and maintenance of the gut barrier (Amin et al., 2009) and S-Adenosylmethionine (SAM) synthesis to positive impacts on depressive symptoms and hepatic protection suggest these microbiome-associated features may be involved in signaling pathways moderating symptom severity in patients with AUD (Cederbaum, 2010).

An increased abundance of Prevotella copri in gut microbiome samples was associated with lower subjective symptom burden including anxiety, depression, and sleep quality scores. Despite consistent associations with Prevotella copri abundance and clinical symptom severity, Prevotella copri was not significantly associated with brain ROI or GBM biomarkers. Interestingly, the association of Prevotella copri abundance with markers of health like glucose response have been conflicting in the literature (Kovatcheva-Datchary et al., 2015; Pedersen et al., 2016), and an increased abundance of this taxon has also been associated with markers of end-organ disease like liver fibrosis (Dong et al., 2020). As the abundance of Prevotella in the gut microbiome has been demonstrated to be strongly influenced by lifestyle choices such as alcohol intake or diet (De Filippis et al., 2016; Kwan et al., 2022), examining interactions between food and alcohol intake in the analysis of clinical phenotype and Prevotella associations may inform the functional role of this bacteria in patients with AUD. Finally, the abundance of Ruminococcus callidus was negatively associated with PSQI scores indicating a positive relationship between abundance of this taxa and improved subjective sleep quality. In other research, patients with AUD who had increased intestinal permeability had a significant decrease in Ruminococcus taxa (Leclercq, Matamoros, et al., 2014), suggesting these taxa may be associated with both improved gastrointestinal barrier function and AUD-associated symptom burden. This preliminary identification of bacterial taxa associated with gut-brain signaling outcomes (i.e., brain morphometry, neuropsychologic symptoms) can potentially inform important study design considerations including sequencing strategy and targeted metabolites involved in GBM pathways and bacterial utilization.

While this study provides a novel exploration of brain morphometrical regions of interest and the gut microbiome, it is not without limitations. This study is based on secondary analysis and resequencing of fecal samples that were collected during the primary microbiome protocol, and the sample size is constrained by the number of patients who had structural MRI images obtained in addition to fecal samples for gut microbiome analysis. This population of individuals with AUD was heterogeneous and may not be completely representative of a general population of individuals with severe AUD. Variables such as the amount of alcohol consumed prior to treatment and demographics are not evenly distributed across this set of patients, and the study cohort did not include control participants. We also understand that having subjects scanned on two different scanners might have limited the effect size of detected structural differences. However, using the data from both scanners expands the generalizability of this model which should be examined with a larger sample size. Although we use GBMs that provide

more insight into gut-brain pathways, the concept of GBMs is still quite new, and therefore, comparisons to other studies using GBMs was limited to the small number of other studies that included GBMs as microbiome-associated biomarkers. Finally, the small sample size prevented the use of advanced statistical modeling or the ability to control for covariates, and bivariate comparisons were used for all statistics. Replication of these measures in study cohorts with larger sample sizes and control participants will be necessary to confirm if the microbiome-associated biomarkers associated with MRI and clinical features found in this analysis can be replicated while controlling for patient-specific factors and providing meaningful clinical inference. Despite the limitations, this study provides a framework to guide future researchers who aim to integrate multimodal features to perform biobehavioral investigations of mechanisms underlying gut-brain signaling and clinical phenotype in patients with AUD

Using structural MRI and gut microbiome features, along with clinical symptom data relevant to AUD, we identified clinically and statistically significant features that can be used to understand altered gut-brain signaling pathways resulting from heavy alcohol use. Although there have been other studies focused on associations between structural MRI brain ROI and gut microbiome data in patients with neuropsychiatric disorders, to our knowledge, this is the first study integrating MRI, microbiome, and clinical features in patients with AUD. Furthermore, capitalizing on a methodology that incorporates multiple components of a neuroactive pathway (Valles-Colomer et al., 2019), the use of GBM pathways as opposed to quantifying individual functional genes enables increased confidence when drawing inferences from this preliminary functional microbiome data. Although we do not vet understand whether pathologic gut-brain signaling precedes heavy alcohol use and increases the risk for AUD, or if these signaling processes are in response to alcohol-associated pathology, we identify preliminary taxonomic and functional microbiome features associated with patient phenotype that can be used to inform mechanistic targets and future interventional research. This work combining results from both MRI and the microbiome in patients with AUD provides limited preliminary gut-brain signaling data, however, these results will help support future longitudinal analyses that may provide a more substantive road map for meaningful clinical inferences. Our hope is the results generated from this research will produce pre-clinical and translational research hypotheses to facilitate continued knowledge and improved health outcomes in patients with AUD.

#### **ACKNOWLEDGMENTS**

We would like to acknowledge and thank the patients for participating in this research, the clinical staff on the 1SE inpatient unit and Ralph Thadeus Tuason for their support of data collection in the primary and secondary studies, John McCulloch from the National Cancer Institute for his advice on running the JAMS program and setting up the Biowulf HPC computing environment at the start of bioinformatics processing for the study, Bing Li for

ALCOHOL & ISB

her assistance with the structural MRI analysis, Andrew S. Burns and the National Institute of Allergy and Infectious Diseases Microbiome Program for their technical and analytical assistance in shotgun metagenomics sequencing, Chelsea Crayton for editorial support, and Carina Carbia for her helpful discussions regarding data interpretation.

#### **FUNDING INFORMATION**

This research was supported by intramural research funds from the National Institutes of Health, Clinical Center, and National Institute on Alcohol Abuse and Alcoholism.

#### CONFLICT OF INTEREST STATEMENT

The authors declare no potential conflicts of interest for the research, authorship, and/or publication of this article.

#### DATA AVAILABILITY STATEMENT

Sequencing data was submitted to SRA with a BioProject ID accession number PRJNA1032029 and a release date of June 1, 2024.

#### DECLARATION

The content is solely the responsibility of the authors and does not necessarily represent the official views of the National Institutes of Health.

#### ORCID

Katherine A. Maki https://orcid.org/0000-0003-4578-960X Vijay A. Ramchandani https://orcid.org/0000-0003-2474-2183

#### REFERENCES

- Ames, N.J., Barb, J.J., Schuebel, K., Mudra, S., Meeks, B.K., Tuason, R.T.S. et al. (2020) Longitudinal gut microbiome changes in alcohol use disorder are influenced by abstinence and drinking quantity. Gut Microbes, 11, 1608–1631.
- Amin, P.B., Diebel, L.N. & Liberati, D.M. (2009) Dose-dependent effects of ethanol and *E.coli* on gut permeability and cytokine production. *The Journal of Surgical Research*, 157, 187–192.
- Barb, J.J., Maki, K.A., Kazmi, N., Meeks, B.K., Krumlauf, M., Tuason, R.T. et al. (2022) The oral microbiome in alcohol use disorder: a longitudinal analysis during inpatient treatment. *Journal of Oral Microbiology*, 14, 2004790.
- Bassett, S.A., Young, W., Fraser, K., Dalziel, J.E., Webster, J., Ryan, L. et al. (2019) Metabolome and microbiome profiling of a stress-sensitive rat model of gut-brain axis dysfunction. *Scientific Reports*, 9, 14026.
- Beghini, F., Mciver, L.J., Blanco-Míguez, A., Dubois, L., Asnicar, F., Maharjan, S. et al. (2021) Integrating taxonomic, functional, and strain-level profiling of diverse microbial communities with bioBakery 3. eLife, 10, e65088.
- Belkaid, Y. & Harrison, O.J. (2017) Homeostatic immunity and the microbiota. *Immunity*, 46, 562–576.
- Bishehsari, F., Magno, E., Swanson, G., Desai, V., Voigt, R.M., Forsyth, C.B. et al. (2017) Alcohol and gut-derived inflammation. *Alcohol Research: Current Reviews*, 38, 163–171.
- Bolger, A.M., Lohse, M. & Usadel, B. (2014) Trimmomatic: a flexible trimmer for Illumina sequence data. *Bioinformatics*, 30, 2114–2120.
- Bustamante, J.M., Dawson, T., Loeffler, C., Marfori, Z., Marchesi, J.R., Mullish, B.H. et al. (2022) Impact of fecal microbiota transplantation on gut bacterial bile acid metabolism in humans. *Nutrients*, 14, 5200.

- Carbia, C., Bastiaanssen, T.F.S., Iannone, L.F., García-Cabrerizo, R., Boscaini, S., Berding, K. et al. (2023) The microbiome-gut-brain axis regulates social cognition & craving in young binge drinkers. *eBio-Medicine*, 89, 104442.
- Carbia, C., Lannoy, S., Maurage, P., López-Caneda, E., O'riordan, K.J., Dinan, T.G. et al. (2021) A biological framework for emotional dysregulation in alcohol misuse: from gut to brain. *Molecular Psychiatry*, 26, 1098–1118.
- Cederbaum, A.I. (2010) Hepatoprotective effects of S-adenosyl-L-methionine against alcohol- and cytochrome P450 2E1-induced liver injury. World Journal of Gastroenterology, 16, 1366–1376.
- Clarke, G., Grenham, S., Scully, P., Fitzgerald, P., Moloney, R.D., Shanahan, F. et al. (2013) The microbiome-gut-brain axis during early life regulates the hippocampal serotonergic system in a sex-dependent manner. *Molecular Psychiatry*, 18, 666–673.
- Critchley, H.D. (2005) Neural mechanisms of autonomic, affective, and cognitive integration. *The Journal of Comparative Neurology*, 493, 154–166.
- Cryan, J.F., O'riordan, K.J., Cowan, C.S.M., Sandhu, K.V., Bastiaanssen, T.F.S., Boehme, M. et al. (2019) The microbiota-gut-brain axis. *Physiological Reviews*, 99, 1877–2013.
- Dale, A.M., Fischl, B. & Sereno, M.I. (1999) Cortical surface-based analysis. I. Segmentation and surface reconstruction. *NeuroImage*, 9, 179-194.
- De Filippis, F., Pellegrini, N., Vannini, L., Jeffery, I.B., La Storia, A., Laghi, L. et al. (2016) High-level adherence to a Mediterranean diet beneficially impacts the gut microbiota and associated metabolome. *Gut*, 65, 1812–1821.
- Desikan, R.S., Ségonne, F., Fischl, B., Quinn, B.T., Dickerson, B.C., Blacker, D. et al. (2006) An automated labeling system for subdividing the human cerebral cortex on MRI scans into gyral based regions of interest. *NeuroImage*, 31, 968–980.
- Dinan, T.G. & Cryan, J.F. (2017) Brain-gut-microbiota axis and mental health. *Psychosomatic Medicine*, 79, 920–926.
- Dong, T.S., Katzka, W., Lagishetty, V., Luu, K., Hauer, M., Pisegna, J. et al. (2020) A microbial signature identifies advanced fibrosis in patients with chronic liver disease mainly due to NAFLD. Scientific Reports, 10, 2771.
- Durand, G.A., Pham, T., Ndongo, S., Traore, S.I., Dubourg, G., Lagier, J.C. et al. (2017) *Blautia massiliensis* sp. nov., isolated from a fresh human fecal sample and emended description of the genus *Blautia*. Anaerobe, 43, 47–55.
- Engen, P.A., Green, S.J., Voigt, R.M., Forsyth, C.B. & Keshavarzian, A. (2015) The gastrointestinal microbiome: alcohol effects on the composition of intestinal microbiota. *Alcohol Research: Current Reviews*, 37, 223–236.
- Erb, I. (2023) Power transformations of relative count data as a shrinkage problem. *Information Geometry*, 6, 327–354.
- Erny, D., Hrabě De Angelis, A.L., Jaitin, D., Wieghofer, P., Staszewski, O., David, E. et al. (2015) Host microbiota constantly control maturation and function of microglia in the CNS. *Nature Neuroscience*, 18, 965–977.
- Ferro, D., Baratta, F., Pastori, D., Cocomello, N., Colantoni, A., Angelico, F. et al. (2020) New insights into the pathogenesis of non-alcoholic fatty liver disease: gut-derived lipopolysaccharides and oxidative stress. Nutrients, 12. https://www.mdpi.com/2072-6643/12/9/2762
- Fiksdal, A., Hanlin, L., Kuras, Y., Gianferante, D., Chen, X., Thoma, M.V. et al. (2019) Associations between symptoms of depression and anxiety and cortisol responses to and recovery from acute stress. *Psychoneuroendocrinology*, 102, 44–52.
- Fischl, B. & Dale, A.M. (2000) Measuring the thickness of the human cerebral cortex from magnetic resonance images. *Proceedings of the National Academy of Sciences of the United States of America*, 97, 11050–11055.

29937175, 2024, 7, Downloaded from https://onlinelibrary.wiley.com/doi/10.1111/acer.15346 by Nat Prov Indonesia, Wiley Online Library on [16/07/2024]. See the Terms

and Condition

and-conditions) on Wiley Online Library for rules of use; OA articles are governed by the applicable Creative Commons License

- Franzosa, E.A., Mciver, L.J., Rahnavard, G., Thompson, L.R., Schirmer, M., Weingart, G. et al. (2018) Species-level functional profiling of metagenomes and metatranscriptomes. *Nature Methods*, 15, 962–968.
- Gilpin, N.W. & Koob, G.F. (2008) Neurobiology of alcohol dependence: focus on motivational mechanisms. *Alcohol Research & Health*, 31, 185–195.
- Grace, S., Rossetti, M.G., Allen, N., Batalla, A., Bellani, M., Brambilla, P. et al. (2021) Sex differences in the neuroanatomy of alcohol dependence: hippocampus and amygdala subregions in a sample of 966 people from the ENIGMA addiction working group. *Translational Psychiatry*, 11, 156.
- Heilig, M., Augier, E., Pfarr, S. & Sommer, W.H. (2019) Developing neuroscience-based treatments for alcohol addiction: a matter of choice? *Translational Psychiatry*, 9, 255.
- Hoban, A.E., Stilling, R.M., Moloney, G., Shanahan, F., Dinan, T.G., Clarke, G. et al. (2018) The microbiome regulates amygdala-dependent fear recall. *Molecular Psychiatry*, 23, 1134–1144.
- Hoban, A.E., Stilling, R.M., Ryan, F.J., Shanahan, F., Dinan, T.G., Claesson, M.J. et al. (2016) Regulation of prefrontal cortex myelination by the microbiota. *Translational Psychiatry*, 6, e774.
- Koob, G.F. & Colrain, I.M. (2020) Alcohol use disorder and sleep disturbances: a feed-forward allostatic framework. Neuropsychopharmacology, 45, 141–165.
- Kovatcheva-Datchary, P., Nilsson, A., Akrami, R., Lee, Y.S., De Vadder, F., Arora, T. et al. (2015) Dietary fiber-induced improvement in glucose metabolism is associated with increased abundance of *Prevotella*. *Cell Metabolism*, 22, 971–982.
- Kwan, S.Y., Jiao, J., Joon, A., Wei, P., Petty, L.E., Below, J.E. et al. (2022) Gut microbiome features associated with liver fibrosis in Hispanics, a population at high risk for fatty liver disease. *Hepatology*, 75, 955–967.
- Langmead, B. & Salzberg, S.L. (2012) Fast gapped-read alignment with bowtie 2. *Nature Methods*, 9, 357–359.
- Lautarescu, A., Craig, M.C. & Glover, V. (2020) Prenatal stress: effects on fetal and child brain development. *International Review of Neurobiology*, 150, 17–40.
- Leclercq, S., Cani, P.D., Neyrinck, A.M., Stärkel, P., Jamar, F., Mikolajczak, M. et al. (2012) Role of intestinal permeability and inflammation in the biological and behavioral control of alcohol-dependent subjects. Brain, Behavior, and Immunity, 26, 911–918.
- Leclercq, S., De Saeger, C., Delzenne, N., DE Timary, P. & Stärkel, P. (2014) Role of inflammatory pathways, blood mononuclear cells, and gut-derived bacterial products in alcohol dependence. *Biological Psychiatry*, 76, 725–733.
- Leclercq, S., Matamoros, S., Cani, P.D., Neyrinck, A.M., Jamar, F., Stärkel, P. et al. (2014) Intestinal permeability, gut-bacterial dysbiosis, and behavioral markers of alcohol-dependence severity. Proceedings of the National Academy of Sciences of the United States of America, 111, E4485–E4493.
- Leclercq, S., Schwarz, M., Delzenne, N.M., Stärkel, P. & De Timary, P. (2021) Alterations of kynurenine pathway in alcohol use disorder and abstinence: a link with gut microbiota, peripheral inflammation and psychological symptoms. *Translational Psychiatry*, 11, 503.
- Li, D., Liu, C.M., Luo, R., Sadakane, K. & Lam, T.W. (2015) MEGAHIT: an ultra-fast single-node solution for large and complex metagenomics assembly via succinct de Bruijn graph. *Bioinformatics*, 31, 1674–1676.
- Liu, X., Mao, B., Gu, J., Wu, J., Cui, S., Wang, G. et al. (2021) Blautia-a new functional genus with potential probiotic properties? *Gut Microbes*, 13, 1–21.
- Luczynski, P., Whelan, S.O., O'sullivan, C., Clarke, G., Shanahan, F., Dinan, T.G. et al. (2016) Adult microbiota-deficient mice have distinct dendritic morphological changes: differential effects in the amygdala and hippocampus. The European Journal of Neuroscience, 44, 2654–2666.

- McCulloch, J.A., Badger, J.H., Cannon, N., Rodrigues, R.R., Valencia, M., Barb, J.J. et al. (2023) JAMS-A framework for the taxonomic and functional exploration of microbiological genomic data. *bioRxiv*, 2023.03. 03.531026. https://doi.org/10.1101/2023.03.03.531026
- Momenan, R., Steckler, L.E., Saad, Z.S., Van Rafelghem, S., Kerich, M.J. & Hommer, D.W. (2012) Effects of alcohol dependence on cortical thickness as determined by magnetic resonance imaging. *Psychiatry Research*. 204, 101–111.
- Ó Cuív, P., De Wouters, T., Giri, R., Mondot, S., Smith, W.J., Blottière, H.M. et al. (2017) The gut bacterium and pathobiont Bacteroides vulgatus activates NF-κB in a human gut epithelial cell line in a strain and growth phase dependent manner. *Anaerobe*, 47, 209–217.
- Pedersen, H.K., Gudmundsdottir, V., Nielsen, H.B., Hyotylainen, T., Nielsen, T., Jensen, B.A. et al. (2016) Human gut microbes impact host serum metabolome and insulin sensitivity. *Nature*, 535, 376–381.
- Pennington, D.L., Durazzo, T.C., Schmidt, T.P., Abé, C., Mon, A. & Meyerhoff, D.J. (2015) Alcohol use disorder with and without stimulant use: brain morphometry and its associations with cigarette smoking, cognition, and inhibitory control. *PLoS One*, 10, e0122505.
- Pinto-Sanchez, M.I., Hall, G.B., Ghajar, K., Nardelli, A., Bolino, C., Lau, J.T. et al. (2017) Probiotic Bifidobacterium longum NCC3001 reduces depression scores and alters brain activity: a pilot study in patients with irritable bowel syndrome. *Gastroenterology*, 153, 448–459.e8.
- Quevedo, K., Doty, J., Roos, L. & Anker, J.J. (2017) The cortisol awakening response and anterior cingulate cortex function in maltreated depressed versus non-maltreated depressed youth. *Psychoneuroendocrinology*, 86, 87–95.
- Reedy, J., Lerman, J.L., Krebs-Smith, S.M., Kirkpatrick, S.I., Pannucci, T.E., Wilson, M.M. et al. (2018) Evaluation of the Healthy Eating Index-2015. Journal of the Academy of Nutrition and Dietetics, 118, 1622–1633.
- Rohleder, N. (2019) Stress and inflammation the need to address the gap in the transition between acute and chronic stress effects. *Psychoneuroendocrinology*, 105, 164–171.
- Senatorov, V.V., Damadzic, R., Mann, C.L., Schwandt, M.L., George, D.T., Hommer, D.W. et al. (2015) Reduced anterior insula, enlarged amygdala in alcoholism and associated depleted von Economo neurons. *Brain*, 138, 69–79.
- Silva, Y.P., Bernardi, A. & Frozza, R.L. (2020) The role of short-chain fatty acids from gut microbiota in gut-brain communication. *Frontiers in Endocrinology*, 11, 25.
- Smith, R.P., Easson, C., Lyle, S.M., Kapoor, R., Donnelly, C.P., Davidson, E.J. et al. (2019) Gut microbiome diversity is associated with sleep physiology in humans. *PLoS One*, 14, e0222394.
- Stilling, R.M., Ryan, F.J., Hoban, A.E., Shanahan, F., Clarke, G., Claesson, M.J. et al. (2015) Microbes & neurodevelopment-absence of microbiota during early life increases activity-related transcriptional pathways in the amygdala. *Brain, Behavior, and Immunity*, 50, 209-220.
- Valles-Colomer, M., Falony, G., Darzi, Y., Tigchelaar, E.F., Wang, J., Tito, R.Y. et al. (2019) The neuroactive potential of the human gut microbiota in quality of life and depression. *Nature Microbiology*, 4, 623-632.
- Volkow, N.D., Koob, G. & Baler, R. (2015) Biomarkers in substance use disorders. ACS Chemical Neuroscience, 6, 522–525.
- Wallen, G.R., Park, J., Krumlauf, M. & Brooks, A.T. (2019) Identification of distinct latent classes related to sleep, Ptsd, depression, and anxiety in individuals diagnosed with severe alcohol use disorder. Behavioral Sleep Medicine, 17, 514–523.
- Wang, S., Harvey, L., Martin, R., Van Der Beek, E.M., Knol, J., Cryan, J.F. et al. (2018) Targeting the gut microbiota to influence brain development and function in early life. *Neuroscience and Biobehavioral Reviews*, 95, 191–201.
- Weber, N., Liou, D., Dommer, J., Macmenamin, P., Quiñones, M., Misner, I. et al. (2018) Nephele: a cloud platform for simplified, standardized



- and reproducible microbiome data analysis. *Bioinformatics*, 34, 1411–1413.
- Witkiewitz, K., Litten, R.Z. & Leggio, L. (2019) Advances in the science and treatment of alcohol use disorder. *Science Advances*, 5, eaax4043.
- Wood, D.E., Lu, J. & Langmead, B. (2019) Improved metagenomic analysis with kraken 2. *Genome Biology*, 20, 257.
- World Health Organization. (2019) Global status report on alcohol and health 2018. Geneva, Switzerland: World Health Organization.
- Xu, M., Lan, R., Qiao, L., Lin, X., Hu, D., Zhang, S. et al. (2023) Bacteroides vulgatus ameliorates lipid metabolic disorders and modulates gut microbial composition in hyperlipidemic rats. *Microbiology Spectrum*, 11, e0251722.
- Yang, X., Tian, F., Zhang, H., Zeng, J., Chen, T., Wang, S. et al. (2016) Cortical and subcortical gray matter shrinkage in alcohol-use disorders: a voxel-based meta-analysis. Neuroscience and Biobehavioral Reviews, 66, 92–103.

#### SUPPORTING INFORMATION

Additional supporting information can be found online in the Supporting Information section at the end of this article.

How to cite this article: Maki, K.A., Wallen, G.R., Bastiaanssen, T.F.S., Hsu, L.-Y., Valencia, M.E., Ramchandani, V.A. et al. (2024) The gut-brain axis in individuals with alcohol use disorder: An exploratory study of associations among clinical symptoms, brain morphometry, and the gut microbiome. *Alcohol: Clinical and Experimental Research*, 48, 1261–1277. Available from: https://doi.org/10.1111/acer.15346